

The color glass condensate and the average transverse momentum in proton-nucleus collisions

F.O. Durães¹, A.V. Giannini², V.P. Gonçalves³ and F.S. Navarra²

¹ Curso de Física, Escola de Engenharia, Universidade Presbiteriana Mackenzie, CEP 01302-907, São Paulo, Brazil

² Instituto de Física, Universidade de São Paulo, CEP 05315-970 São Paulo, SP, Brazil

³ Instituto de Física e Matemática, Universidade Federal de Pelotas, CEP 96010-900, Pelotas, RS, Brazil

E-mail: duraes@mackenzie.br

E-mail: avgiannini@usp.br

E-mail: victorpb@gmail.com

E-mail: navarra@if.usp.br

Abstract.

We compute the energy and rapidity dependence of the average transverse momentum $\langle p_T \rangle$ in pp and pA collisions at RHIC and LHC energies in the framework of the Color Glass Condensate (CGC) formalism. We update previous predictions for the p_T - spectra using the hybrid formalism of the CGC approach and two phenomenological models for the dipole - target scattering amplitude. We demonstrate that these models are able to describe the RHIC and LHC data for the hadron production in pp , dAu and pPb collisions at $p_T \leq 20$ GeV. Moreover, we present our predictions for $\langle p_T \rangle$ and demonstrate that the ratio $\langle p_T(y) \rangle / \langle p_T(y=0) \rangle$ decreases with the rapidity and has a behavior similar to that predicted by hydrodynamical calculations.

1. Introduction

In the LHC experiments we can study several aspects of *forward physics* as, for instance, soft and hard diffraction, exclusive production of new mass states, low- x dynamics and other important topics [1]. Forward physics is characterized by the production of particles with relatively small transverse momentum, being traditionally associated with soft particle production, which is intrinsically non perturbative and not amenable to first-principles analysis. However, in particle production at large energies and forward rapidities, the wave function of one of the projectiles is probed at large Bjorken x and that of the other at very small x . The latter is characterized by a large number of gluons, which is expected to form a new state of matter - the Color Glass Condensate (CGC) - where the gluon distribution saturates and non linear phenomena dominate. Such a system is endowed with a new dynamical momentum scale, the saturation scale Q_s , which controls the main features of particle production. At large energies and rapidities, Q_s is expected to become much larger than the QCD confinement scale Λ_{QCD} . Furthermore, the saturation scale is expected to determine the typical transverse momentum of the produced partons in the interaction.



In a recent paper [2] it was suggested that the analysis of $\langle p_T \rangle$ in pp and pA collisions can be used to disentangle the hydrodynamical and the CGC descriptions of the “ridge” effect observed in high multiplicity events in small colliding systems such as pp and $p(d)A$. While the ridge-type structure previously observed in heavy-ion collisions at RHIC and the LHC was considered as an evidence of the hydrodynamical nature of the quark-gluon-plasma, there is no compelling reason why small systems should also exhibit a hydrodynamical behavior even though a hydro approach is able to describe the experimental data. On the other hand, the CGC approach also provides a qualitatively good description of the same data. Therefore, the origin of the ridge in pp and pA collisions is still an open question. Like the ridge effect, the azimuthal asymmetries observed in pPb collisions at the LHC energies can also be understood with different theoretical explanations. While in the hydro approaches those anisotropies emerge as a final state feature due to the hydrodynamic flow, in the CGC approach they are described as a initial state anisotropies which are present at the earliest stages of the collision.

In Ref. [2], the authors have studied the rapidity (y) dependence of the average transverse momentum of charged particles using very general arguments that lead to simple analytical expressions. In particular, the Golec - Biernat – Wusthoff (GBW) model [3] was used to describe the unintegrated gluon distribution and the fragmentation of the partons into final state particles was neglected. The authors of [2] have found that the average transverse momentum $\langle p_T \rangle$ in the CGC approach grows with rapidity, in contrast to what is expected from a collective expansion. Indeed, the hydrodynamical model predicts a decrease of the average transverse momentum when going from midrapidity, $y = 0$, to the proton side, owing to a decreasing number of produced particles. These different predictions of the hydrodynamical and CGC approaches motivate us to perform a more careful analysis of the energy and rapidity dependencies of $\langle p_T \rangle$. As the GBW model does not describe the p_T - spectra measured in pp/pA collisions, in our study we will consider two more realistic phenomenological saturation models that are able to reproduce the experimental data in the region of small transverse momenta. This is the region that determines the behavior of the average transverse momentum. Moreover, we will analyse the impact of the inclusion of parton fragmentation in the rapidity dependence of $\langle p_T \rangle$. With these improvements, we are able to present realistic predictions for $\langle p_T \rangle$ based on the CGC results that are able to describe the current experimental data on hadron production in hadronic collisions.

2. Particle production in the CGC hybrid formalism

Forward hadron production in hadron-hadron collisions is a typical example of a dilute-dense process [4] which is an ideal system to study the small- x components of the target wave function. In this case the cross section is expressed as a convolution of the standard parton distributions for the dilute projectile, the dipole-hadron scattering amplitude (which includes the high-density effects) and the parton fragmentation functions. Basically, assuming this generalized dense-dilute factorization, the minimum bias invariant yield for single-inclusive hadron production in hadron-hadron processes is described in the CGC formalism by [5]

$$\begin{aligned} \frac{dN_h}{dyd^2p_T} = & \frac{K(y)}{(2\pi)^2} \int_{x_F}^1 dx_1 \frac{x_1}{x_F} \left[f_{q/p}(x_1, \mu^2) \tilde{\mathcal{N}}_F \left(\frac{x_1}{x_F} p_T, x_2 \right) D_{h/q} \left(\frac{x_F}{x_1}, \mu^2 \right) \right. \\ & \left. + f_{g/p}(x_1, \mu^2) \tilde{\mathcal{N}}_A \left(\frac{x_1}{x_F} p_T, x_2 \right) D_{h/g} \left(\frac{x_F}{x_1}, \mu^2 \right) \right], \end{aligned} \quad (1)$$

where p_T , y and x_F are the transverse momentum, rapidity and the Feynman- x of the produced hadron, respectively. The $K(y)$ -factor mimics the effect of higher order corrections and, effectively, that of other dynamical effects not included in the CGC formulation. The variable x_1 denotes the momentum fraction of a projectile parton, $f(x_1, \mu^2)$ the projectile parton distribution

functions and $D(z, \mu^2)$ the parton fragmentation functions into hadrons. These quantities evolve according to the DGLAP evolution equations and obey the momentum sum-rule. It is useful to assume $\mu^2 = p_T^2$. Moreover, $x_F = \frac{p_T}{\sqrt{s}} e^y$ and the momentum fraction of the target partons is given by $x_2 = x_1 e^{-2y}$ (For details see e.g. [5]). In Eq. (1), $\widetilde{\mathcal{N}}_F(x, k)$ and $\widetilde{\mathcal{N}}_A(x, k)$ are the fundamental and adjoint representations of the forward dipole amplitude in momentum space and are given by

$$\widetilde{\mathcal{N}}_{A,F}(x, p_T) = \int d^2r e^{ip_T \cdot \vec{r}} [1 - \mathcal{N}_{A,F}(x, r)] , \quad (2)$$

where $\mathcal{N}_{A,F}(x, r)$ encodes all the information about the hadronic scattering, and thus about the non-linear and quantum effects in the hadron wave function. Following [6], we will assume in what follows that $\mathcal{N}_F(x, r)$ can be obtained from $\mathcal{N}_A(x, r)$ after rescaling the saturation scale by $Q_{s,F}^2 = (C_F/C_A)Q_{s,A}^2$ where $C_F/C_A = 4/9$. We will consider two different phenomenological models based on the analytical solutions of this equation. This allows us to investigate the possibility of getting a first insight on whether or not the LHC data are sensitive to geometric scaling violations at high values of p_T . Moreover, as these phenomenological models differ from the GBW model in the dependence of the anomalous dimension with the momentum scale (see below), it becomes possible to clarify the origin of the differences between the predictions.

Several groups have constructed phenomenological models for the dipole scattering amplitude using the RHIC and/or HERA data to fix the free parameters [5, 6, 7, 8]. In general, it is assumed that \mathcal{N} can be modelled through a simple Glauber-like formula,

$$\mathcal{N}(x, r_T) = 1 - \exp \left[-\frac{1}{4} (r_T^2 Q_s^2)^\gamma \right] , \quad (3)$$

where γ is the anomalous dimension of the target gluon distribution. The speed with which we move from the non linear regime to the extended geometric scaling regime and then from the latter to the linear regime is what differs one phenomenological model from another. This transition speed is dictated by the behavior of the anomalous dimension $\gamma(x, r_T^2)$. In the GBW model, γ is assumed to be constant and equal to one. In this paper we will consider the dipole models proposed in Refs. [5, 6] to describe the p_T spectra of particles produced at RHIC. In the DHJ model [5], the anomalous dimension is given by

$$\gamma(x, r_T)_{DHJ} = \gamma_s + (1 - \gamma_s) \frac{|\log(1/r_T^2 Q_s^2)|}{\lambda y + d\sqrt{y} + |\log(1/r_T^2 Q_s^2)|} . \quad (4)$$

with $Q_s^2 = A^{1/3} Q_0^2 (x_0/x_2)^\lambda$, $\gamma_s = 0.628$, $Q_0^2 = 1.0 \text{ GeV}^2$, $x_0 = 3.0 \cdot 10^{-4}$, $\lambda = 0.288$ and $d = 1.2$. This model was designed to describe the forward dAu data at the highest RHIC energy taking into account geometric scaling violations characterized by terms depending on the target rapidity, $y = \log(1/x_2)$, in its parametrization of the anomalous dimension, with the parameter d controlling the strength of the subleading term in y . In contrast, in the BUW model [6] the anomalous dimension is given by

$$\gamma(\omega = q_T/Q_s)_{BUW} = \gamma_s + (1 - \gamma_s) \frac{(\omega^a - 1)}{(\omega^a - 1) + b} , \quad (5)$$

where $q_T = p_T/z$ is the parton momentum. The parameters of the model ($\gamma_s = 0.628$, $a = 2.82$ and $b = 168$) have been fixed by fitting the p_T -spectra of the produced hadrons measured in pp and dAu collisions at RHIC energies. With these parameters the model was also able to describe the ep HERA data for the proton structure function if the light quark masses are neglected. An

important feature of this model is the fact that it explicitly satisfies the property of geometric scaling. Since the forward RHIC data on p_T -spectra are reproduced by both models [6, 5], it was not possible to say whether experimental data show violations of the geometric scaling or not. In principle, it is expected that by considering the transverse momentum distribution of produced hadrons measured at the LHC energies it should be possible to address this question since the new data are taken at a wider range of p_T when compared to the RHIC data.

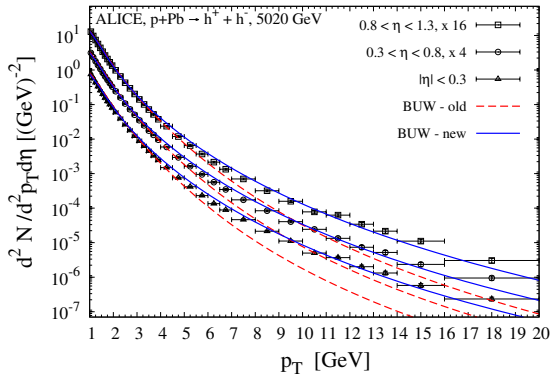


Figure 1. Comparison between the BUW predictions for the transverse momentum p_T -spectra of charged particles produced in pPb collisions and the ALICE data [9].

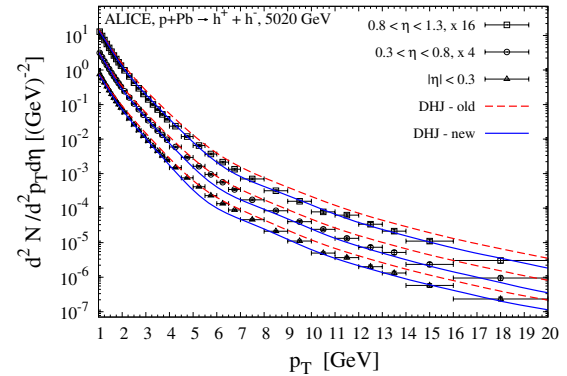


Figure 2. Comparison between the DHJ predictions for the transverse momentum p_T -spectra of charged particles produced in pPb collisions and the ALICE data [9].

3. Results and discussion

In what follows we will present our results for the average transverse momentum $\langle p_T \rangle$ defined by

$$\langle p_T \rangle = \frac{\int d^2 p_T p_T \frac{dN_h}{dy d^2 p_T}}{\int d^2 p_T \frac{dN_h}{dy d^2 p_T}} \quad (6)$$

which is rapidity and energy dependent, i.e. $\langle p_T \rangle = \langle p_T(y, \sqrt{s}) \rangle$. In order to obtain realistic predictions at LHC energies it is fundamental to use a model, which can describe the experimental data on the p_T – spectra of produced particles, as input in the calculations. Consequently, as the first step we will initially compare the DHJ and BUW predictions with the recent LHC data. In Figs. 1 and 2 we present a comparison of these predictions using the original parameters, denoted “DHJ old” and “BUW old” in the figures, with the LHC data on the p_T – spectra of charged particles in pPb collisions at $\sqrt{s} = 5.02$ TeV and different rapidities [9]. We use the CTEQ5L parton distribution functions [10] and the KKP fragmentation functions [11]. Moreover, we compute Eq. (1) using the central values of η in the pseudorapidity ranges used in the experiment and choose $A \equiv A_{\text{min. bias}} = 20$ (18.5) for pPb (dAu) collisions. We find that these models are not able to describe the ALICE data [9] at large transverse momentum with their original parameters and a reanalysis of data is required. We have then determined the free parameters of the BUW and the DHJ dipole scattering amplitudes by fitting the p_T spectra of charged particles measured in pPb collisions at $\sqrt{s} = 5020$ GeV and then compared the updated models with the experimental data on pp collisions at other energies and rapidities. Moreover, differently from the authors of Refs. [5, 6], who have assumed that $\gamma_s \approx 0.63$, which is

the value obtained from the leading order BFKL kernel, we will consider γ_s as a free parameter. The resulting fits are shown in Figs. 1 and 2 for the following parameters: $a = 2.0$, $b = 125$ and $\gamma_s = 0.74$ for the BUW model and $d = 1.0$ and $\gamma_s = 0.7$ for the DHJ model. The data are better described if we assume larger values of $\gamma_s \geq 0.7$, which is consistent with the results obtained using the renormalization group improved BFKL kernels at next-to-leading order and fixed running coupling. As it can be seen, with these parameter sets our curves agree well with the experimental data. In the range $4 < p_T < 7$ GeV the DHJ curves show an “edgy” behaviour which is a reminiscence of the numerical Fourier transform. This is not a big effect and can be considered as part of the theoretical error in our calculations. It is important to emphasize that $\langle p_T \rangle$ is only marginally affected by these small oscillations (see below) and the fits presented here for both models considered are sufficient to get a realistic prediction for this observable since it is dominated by the low p_T region.

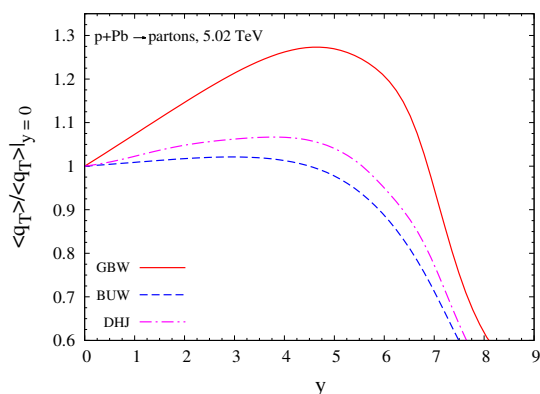


Figure 3. Ratio $\langle p_T(y, \sqrt{s}) \rangle / \langle p_T(0, \sqrt{s}) \rangle$ with different models of forward scattering amplitude in pPb collisions. Parton fragmentation is not included.

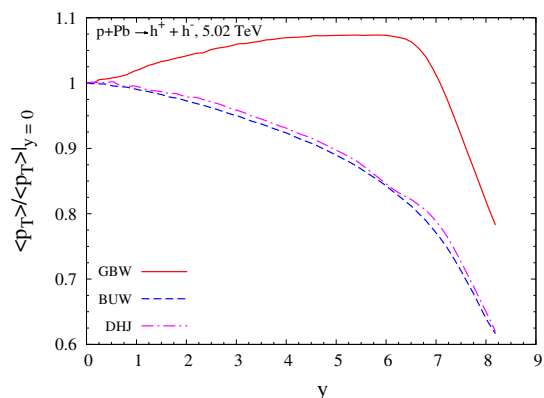


Figure 4. Ratio $\langle p_T(y, \sqrt{s}) \rangle / \langle p_T(0, \sqrt{s}) \rangle$ with different models of forward scattering amplitude in pPb collisions. Parton fragmentation is included.

The results presented in Figs. 1 and 2 make us confident to obtain realistic predictions for the average transverse momentum. In what follows we will study the energy and rapidity dependencies of the ratio

$$R = \frac{\langle p_T(y, \sqrt{s}) \rangle}{\langle p_T(0, \sqrt{s}) \rangle} \quad (7)$$

where the denominator represents the average transverse momentum at zero rapidity. Initially, let us analyse the dependence of our predictions on the model used to describe the forward scattering amplitudes $\mathcal{N}_{\mathcal{A}, \mathcal{F}}(x, r)$ and the impact of the inclusion of parton fragmentation. In Figs. 3 and 4 we compare the predictions of the BUW and DHJ models with those from the GBW model [3], obtained assuming $p_{T, \min} = 1$ GeV. The GBW model is not able to describe the experimental data on hadron production in hadronic collisions. However, as this model is usually considered to obtain analytical results for several observables, we would like to verify if its predictions for $\langle p_T \rangle$ are realistic. In Fig. 3 we present our predictions disregarding parton fragmentation, while in Fig. 4 fragmentation is included. It is important to emphasize that our results for the GBW model without fragmentation, obtained using the hybrid formalism are similar to those obtained in Ref. [2] with the k_T - factorization approach. We can see that the DHJ and BUW predictions are similar (to each other) and differ significantly from the GBW one. While the GBW model predicts a growth of the ratio for $y \leq 6$, the BUW and DHJ models predict that this ratio is almost constant or decreases with rapidity. The inclusion

of parton fragmentation modifies the rapidity dependence, implying a smaller growth of the GBW prediction. In the case of the DHJ and BUW predictions, the inclusion of fragmentation implies that the fall of the ratio begins at smaller rapidities. Our results demonstrate that the inclusion of fragmentation has an important impact on the behavior of $\langle p_T \rangle$. However, the main difference between our predictions and those presented in Ref. [2] comes from the model used to describe the QCD dynamics at high energies. This distinct behavior is present for pp and pPb collisions, with the behavior of the ratio at very large rapidities being determined by kinematical constraints associated to the limited phase space.

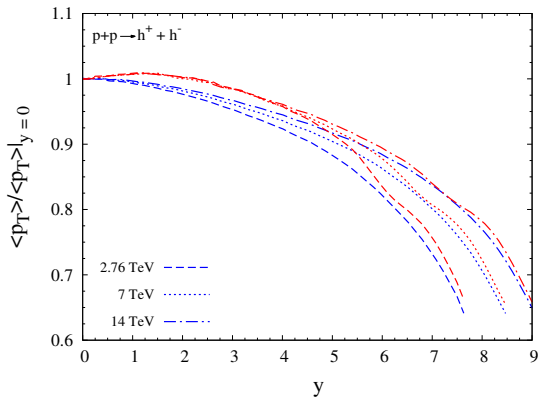


Figure 5. Rapidity dependence of the ratio $R = \langle p_T(y, \sqrt{s}) \rangle / \langle p_T(0, \sqrt{s}) \rangle$ in pp collisions for different energies. The BUW (DHJ) predictions are represented by blue (red) lines.

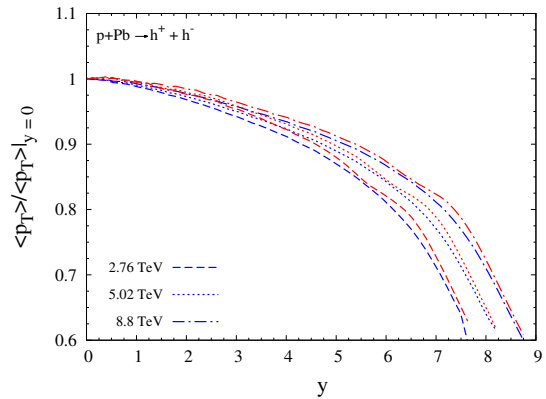


Figure 6. Rapidity dependence of the ratio $R = \langle p_T(y, \sqrt{s}) \rangle / \langle p_T(0, \sqrt{s}) \rangle$ in pPb collisions for different energies. The BUW (DHJ) predictions are represented by blue (red) lines.

In Figs. 5 and 6 we present the behavior of the ratio $\langle p_T(y, \sqrt{s}) \rangle / \langle p_T(0, \sqrt{s}) \rangle$ for pp and pPb collisions considering different center of mass energies. We find that the predictions of the DHJ (red lines) and BUW (blue lines) are similar, with the DHJ being slightly larger than the BUW, and that the ratio increases with energy. The results from Figs. 5 and 6 indicate that the ratio R decreases with the rapidity in pPb collisions for the energies probed by LHC, presenting a behavior similar to that obtained using a hydrodynamical approach, which implies that this observable cannot be used to discriminate the CGC and hydrodynamical approaches for the description of the high multiplicity events. This conclusion is opposite to that obtained in Ref. [2]. This difference comes from several facts. First, the CGC results in Ref. [2] were obtained using an analytical approximation for a particular unintegrated gluon distribution that does not describe (even at a qualitative level) the experimentally measured p_T -spectra. Second, the calculation presented in [2] does not include the important contribution of the fragmentation processes to the average transverse momentum. Finally, kinematical constraints associated with phase space restrictions at large rapidities were not included in [2] and, even in a partonic scenario, they play an important role at very large rapidities. In contrast, in our analysis we have calculated the ratio R using two different models for the forward scattering amplitude that are able to describe the current experimental data on charged hadron and pion p_T spectra measured in pp and pPb collisions at LHC. We have included the effects of parton fragmentation and phase space restrictions. It is important to emphasize that although we have used the hybrid formalism instead of the k_T -factorization approach, we have verified that both approaches imply a similar behavior for the ratio R when the GBW model is used as input and the parton fragmentation is not taken into account. Our results demonstrate that the main difference comes from the treatment of the QCD dynamics at high energies.

4. Conclusions

We have considered the hybrid formalism to study the behavior of the average p_T with respect to the rapidity in pp and pPb collisions at several energies in the CGC picture of high energy collisions. In order to obtain realistic predictions we have updated previous phenomenological models for the forward scattering amplitude, one with and other without geometric scaling violations. After constraining their parameters with the most recent data on the p_T spectra of charged particles measured in pPb collisions at the LHC, we have demonstrated (see details in Ref.[12]) that they are able to describe the recent pp data on the charged hadron and pion p_T spectra measured at the LHC in the kinematical range of $p_T \leq 20$ GeV. Using these models as input, we have calculated the average transverse momentum $\langle p_T(y, \sqrt{s}) \rangle$ in pp and pPb collisions, and estimated the energy and rapidity dependencies of the ratio $R = \frac{\langle p_T(y, \sqrt{s}) \rangle}{\langle p_T(0, \sqrt{s}) \rangle}$. We have demonstrated that this ratio increases with the energy for a fixed rapidity and decreases with the rapidity for a fixed energy, which is similar to the predication of hydrodynamical approaches for high multiplicity events. Our results indicated that this decreasing comes from the treatment of the QCD dynamics at high energies and the inclusion of the fragmentation process and kinematical constraints associated to the phase space restrictions at very large rapidities.

Acknowledgments

This work was partially financed by the Brazilian funding agencies CAPES, CNPq, FAPESP and FAPERGS.

References

- [1] F. Gelis, E. Iancu, J. Jalilian-Marian and R. Venugopalan, Ann. Rev. Nucl. Part. Sci. **60**, 463 (2010); K. J. Golec-Biernat and M. Wusthoff, Phys. Rev. D **59**, 014017 (1998); M. S. Kugeratski, V. P. Goncalves and F. S. Navarra, Eur. Phys. J. C **46**, 413 (2006).
- [2] P. Bozek, A. Bzdak and V. Skokov, Phys. Lett. B **728**, 662 (2014).
- [3] K. J. Golec-Biernat, M. Wusthoff, Phys. Rev. D **59**, 014017 (1998).
- [4] E. Iancu, C. Marquet and G. Soyez, Nucl. Phys. A **780**, 52 (2006).
- [5] A. Dumitru, A. Hayashigaki and J. Jalilian-Marian, Nucl. Phys. A **765**, 464 (2006); Nucl. Phys. A **770**, 57 (2006).
- [6] D. Boer, A. Utermann, E. Wessels, Phys. Rev. D **77**, 054014 (2008).
- [7] D. Kharzeev, Y.V. Kovchegov and K. Tuchin, Phys. Lett. B **599**, 23 (2004).
- [8] J. Bartels, K. Golec-Biernat, H. Kowalski, Phys. Rev. D **66**, 014001 (2002); H. Kowalski and D. Teaney, Phys. Rev. D **68**, 114005 (2003); E. Iancu, K. Itakura, S. Munier, Phys. Lett. B **590**, 199 (2004); H. Kowalski, L. Motyka and G. Watt, Phys. Rev. D **74**, 074016 (2006); V. P. Goncalves, M. S. Kugeratski, M. V. T. Machado and F. S. Navarra, Phys. Lett. B **643**, 273 (2006); C. Marquet, R. Peschanski and G. Soyez, Phys. Rev. D **76**, 034011 (2007); G. Soyez, Phys. Lett. B **655**, 32 (2007); G. Watt and H. Kowalski, Phys. Rev. D **78**, 014016 (2008).
- [9] B. Abelev *et al.* [ALICE Collaboration], Phys. Rev. Lett. **110**, 082302 (2013).
- [10] H. L. Lai *et al.* [CTEQ Collaboration], Eur. Phys. J. C **12**, 375 (2000).
- [11] B.A. Kniehl, G. Kramer and B. Pötter, Nucl. Phys. B **582**, 514 (2000).
- [12] F. O. Durães, A. V. Giannini, V. P. Goncalves and F. S. Navarra, arXiv:1510.04737 [hep-ph].